

<https://doi.org/10.1038/s41522-025-00723-9>

The role of gut microbiota-gonadal axis in ovary activation of Asian honey bee (*Apis cerana*) queens



Chonghui Zhao^{1,2,6}, Yehua Peng^{2,3,6}, Wenfeng Li^{2,6}✉, Muhammad Fahad Raza², Wenbo Wang^{2,3}, Yi Zhang⁴, Yanping Chen⁵, Jun Guo¹✉, Shaokang Huang³✉ & Richou Han²✉

The gut microbiota-gonadal axis is increasingly recognized, but its reproductive roles remain unclear. Here, we used the Asian honey bee *Apis cerana* queens as a model to investigate the role of the gut microbiota-gonadal axis on ovary activation. By artificially caging and releasing the mated queens for a short or long period and monitoring the morphological changes of their ovaries, we confirmed that the activation and suppression of the queen ovary could be switched quickly. We found that the ovary weight was positively correlated with the body weight. 16S rRNA sequencing showed ovarian deactivation reduced gut *Lactobacillus* abundance. Untargeted metabolomics identified purine metabolism as the dominant ovarian pathway, while correlation analyses implicated *Lactobacillus* in modulating ovarian morphology through purine signaling. This study elucidates microbiota-gonadal crosstalk governing reproduction, providing mechanistic insights with translational potential for reproductive health management.

Gut microbiota have complex interactions with distant organs and play a crucial role in various physiological processes, including reproductive functions. Previous studies showed that the gut microbiota could regulate and be influenced by the level of gonadal development, leading to the concept of the gut microbiota-gonadal axis¹. The effect of the gut microbiota on reproduction is rapidly gaining widespread attention^{2,3}. Existing studies have all confirmed the existence and importance of the gut microbiota-gonadal axis in reproduction⁴. On the other hand, gut microbiota dysbiosis can cause ovarian damage, impair fertility, affect oocyte development, disrupt the estrous cycle, and lead to abnormal ovulation⁵. For example, changes in *Drosophila* gut microbiota impacted reproduction, and the removal of gut bacteria, particularly *Acetobacter* species, inhibited oogenesis⁶. In mice, the antibiotic amoxicillin induced dysbiosis of the intestinal flora, altered the estrous cycle, and reduced oocyte numbers. Furthermore, transplantation of fecal bacteria from female mice with ovarian disease led to ovarian dysfunction and impaired fertility⁷. In human females, ovarian insufficiency is strongly associated with disturbances in the intestinal flora⁸.

Conversely, maintaining a healthy gut microbiota enhances the reproductive potential and ensures normal ovarian development. Treating rats with polycystic ovary syndrome (PCOS) using *Lactobacillus* and fecal

microbiota from healthy rats restored the estrous cycle, reduced androgen biosynthesis, and normalized ovarian morphology⁹. Transplanting gut microbiota from young to aged mice significantly improved ovarian function and fertility in the latter by shifting gut composition toward a younger profile, reducing inflammation, and enhancing ovarian health. These findings highlight the potential of gut microbiota modulation to delay ovarian aging¹⁰. In black rhinos, many members of the gut microbiota were significantly associated with reproductive success and ovarian cycle stage, with certain rare species of microbiota playing a particularly important role¹¹. The gut microbiota is linked to female ovarian function through complex mechanisms, which are still largely unknown and require further explorations using various animal models.

Honey bee (genus *Apis*) colonies are matrilineal societies where the queen is the only fertile female and dominates the egg-laying process. In addition, by producing a pheromone, the queen controls many aspects of worker behaviors and colony organization. Therefore, the queen's health is crucial for the overall health of the colony and one of major concerns for beekeepers worldwide.

A virgin queen reaches sexual maturity 7–10 days after emerging from her cell, at which point she initiates mating flights. Over the next few days,

¹Faculty of Life Science and Technology, Kunming University of Science and Technology, Kunming, Yunnan, China. ²Guangdong Key Laboratory of Animal Conservation and Resource Utilization, Guangdong Public Laboratory of Wild Animal Conservation and Utilization, Institute of Zoology, Guangdong Academy of Sciences, Guangzhou, China. ³College of Bee Science and Biomedicine, Fujian Agriculture and Forestry University, Fuzhou, China. ⁴School of Chinese Medicinal Resource, Guangdong Pharmaceutical University, Yunfu, China. ⁵USDA-ARS Bee Research Laboratory, Beltsville, MD, USA. ⁶These authors contributed equally: Chonghui Zhao, Yehua Peng, Wenfeng Li. ✉e-mail: wfliee@giz.gd.cn; guojun0591@126.com; skhuang@fafu.edu.cn; hanrc@giz.gd.cn

she will undertake one to three mating flights, during which she will mate with an average of 12 drones¹². A fully inseminated queen holds around 5–7 million sperm that she uses to fertilize eggs over her lifetime¹³. Once the queen has completed the mating process, she will begin laying eggs in a few days.

During the first days after emergence, the queen's ovary are arrested in previtellogenic stages until mating. Shortly thereafter, the oogenesis is initiated: numerous follicles transition to the vitellogenin phase, and terminal filaments in ovarioles are considerably elongated¹⁴. Her ovaries become enlarged, matuated, and activated. Then the queen starts laying eggs, and the egg-laying rate soon reaches 1500 or more eggs per day.

However, under natural conditions, the egg-laying rate of the queen bee cannot always be maintained at a high level; it fluctuates with seasonal changes¹⁵. Physiologically, this phenomenon manifests as ovarian activation being dynamically regulated¹⁶. Under some seasonal conditions, the queen's ovaries become completely inactive, and oviposition stops. For example, during several weeks in the winter in temperate climates, the queen ceases to lay eggs, and has smaller and less developed ovaries, indicating that ovarian activation is generally suppressed^{17,18}. Although the factors and mechanisms regulating the queen bee's ovarian activation and egg-laying behavior are not yet clear, the photoperiod is considered the most likely external factor. Additionally, pollen collection activity may also play a role, and the internal factor, the filling of the spermatheca, also has an impact¹⁵. On the other hand, queen ovarian activation and oviposition are also regulated by beekeeping management measures such as brood interruption for *Varroa* control and the mailing of queen bees, which usually deactivate the ovary for a period by queen caging^{19–21}. One of the notable features of ovarian activation regulation is the rapid switching between activation and inhibition states within a short period. Thus, regardless of whether the ovarian inhibition is caused by natural or artificial factors, when external conditions change, the ovaries quickly reactivate, and the queen promptly resumes egg-laying.

The molecular mechanisms underlying queen ovarian activation and oviposition have attracted increasing attention. Early studies have focused on the identification of candidate genes and pathways that regulate ovarian development and activation by gene expression profiling. Several genes like *RpL26* (a ribosomal protein), *AmTyr1* (a tyramine receptor gene), *MRJP-3* (a major jelly protein), and *Vit* (vitellogenin) have been found differentially expressed after the CO₂ narcosis treatment, which causes the ovarian activation in queen bees²². Using high-throughput RNA sequencing (RNA-seq) technology, a set of differentially expressed genes has been revealed to activate both queen and worker ovaries²³. Recently, non-coding RNAs, including microRNAs (miRNAs), long non-coding RNAs (lncRNAs), and circular RNAs (circRNAs), have emerged as crucial regulators in various biological processes²⁴. There are a substantial number of miRNAs, lncRNAs, and circRNAs found to be differently expressed during queen ovarian activation, and functional annotation suggests that several pathways like hippo, MAPK, Wnt, FoxO, insulin secretion, and calcium signaling are closely related to this process^{16,25,26}. Most recently, using widely targeted metabolomics has helped identify remarkable metabolite alterations after queen ovarian activation and oviposition: levels of carnitines, fatty acids, and some antioxidants are up-regulated, while the levels of amino acids are significantly down-regulated²⁷. Although the application of advanced technologies has greatly enhanced the understanding of the molecular mechanisms of queen ovarian activation, the overall molecular regulatory network of this process remains unclear.

From the hologenomic perspective, queen bee ovarian activation may also be regulated by its gut microbiome in addition to natural environmental factors. The gut microbiota of worker bees comprises five core bacteria, *Snodgrassella*, *Gilliamella*, *Bifidobacterium*, *Bombilactobacillus*, and *Lactobacillus*²⁸. These bacteria are abundant and stable in the intestines of nearly all healthy worker bees. In contrast, the queen bee's microbiota differs from worker bees. The core microbiota of queen bees includes *Lactobacillus* Firm5, *Lactobacillus* Firm4, *Commensalibacter* (Alpha 2.1), *Bifidobacterium* spp. and *Bombella apis* (Alpha 2.2)^{29–32}.

The gut microbiota of queen bees is dynamic and adaptable, influenced by factors, such as genetic background, age and environment. Genetic background plays a significant role in shaping the queen bee's gut microbiota. The dominant genera in the gut flora of the asexual hybrid queens, bred by trophic hybridization (a queen produced in *A. mellifera* but reared by *A. cerana* nurse bees), are *Brevundimonas*, *Bombella*, and *Lactobacillus*, showing a microbial structure more strongly related to *A. mellifera* queens³³. Age-wise, in the midgut and ileum in both ecological niches, Proteobacteria are more abundant in older queens, while both *Lactobacillus* and *Bifidobacterium* decrease with age³⁴. Season also influences the structure of the gut flora in *Bombus terrestris* queens. The bacterial community composition shows higher OTU richness and homogeneity, with decreased levels of the core bacteria *Gilliamella* and *Snodgrassella*, and an increased relative abundance of non-core bacteria, including several psychrophilic and psychrotrophic taxa³⁵.

Significant differences have been found between the gut microbiomes of virgin and mated bumble bee queens, with an increase in *Bacillus*, *Lactococcus*, and *Pseudomonas* observed after mating³⁶. However, the involvement of the gut microbiota in sexual maturation in queen bees has not been investigated. The queen's gut microbial community responds to changes in reproductive behavior associated with ovarian function, and the reproductive division of labor affects the composition of the gut microbiota²⁹. All of the above studies were conducted under natural conditions, but the interaction between gut microbiota and reproduction needs to be confirmed through more controlled experiments involving human intervention. Powell et al. found that using queen cages to restrict queen laying significantly altered the structure of the gut microbiota³⁷. Recently, a 21-day oviposition restriction treatment has been applied to 1-year-old queen bees, resulting in an increase in *Lactobacillus* and a decrease in *Bombella*³⁸.

Therefore, it is feasible to study the interaction between the gut microbiota and the ovary using the queen bee as a model. Specifically, in this study, we investigated the role of the gut microbiota-gonadal axis in the ovarian activation of *A. cerana* queens. The Asian honey bee, *A. cerana*, is native to Asia and co-exists with the European honey bee, *A. mellifera*, in the region³⁹. It plays a crucial role in both agricultural production and ecological health. Unlike *A. mellifera*, the *A. cerana* queens exhibit several reproductive characteristics: (1) The vagina of the *A. cerana* queen lacks a closed valve fold, making instrumental insemination easier than that in *A. mellifera*⁴⁰; (2) Successful mating flights of the *A. cerana* queen are much longer than those of the *A. mellifera* queen⁴¹; (3) *A. cerana* queens must mate with more drones to ensure complete fertilization⁴⁰. However, compared to *A. mellifera*, the reproductive biology of *A. cerana* queens has been less investigated, leaving many gaps, including the biological processes and regulation of ovarian activation, as well as the interaction between gut microbiota and the ovary. Therefore, the current study focuses on addressing these gaps. In this study, we regulated ovarian activation, development, and recovery by caging *A. cerana* queens and recorded changes in ovarian morphology and queen body weight. Based on metabolomics and microbiomics, we revealed the possible mechanisms of interactions between gut microbiota and ovarian function and provided an important foundation for research on the gut microbiota-gonadal axis in queens. The queen is the primary reproducer of a colony, and her reproductive health is fundamental to colony growth. Studying the interaction between gut microbiota and reproduction makes it possible to promote egg laying by optimizing gut bacteria, which has practical application value for colony management and the sustainable development of beekeeping. It also has the potential to inform future research on reproductive health and disease management in animals and humans, leading to new clinical practices and intervention strategies.

Results

Regulation of queen ovaries by caging

To investigate the effects of restricting queen mating and egg laying on the ovaries, we captured microscopic images of the ovarian morphology (Fig. 1a). We measured the weight of the queens' ovaries (Fig. 1b and

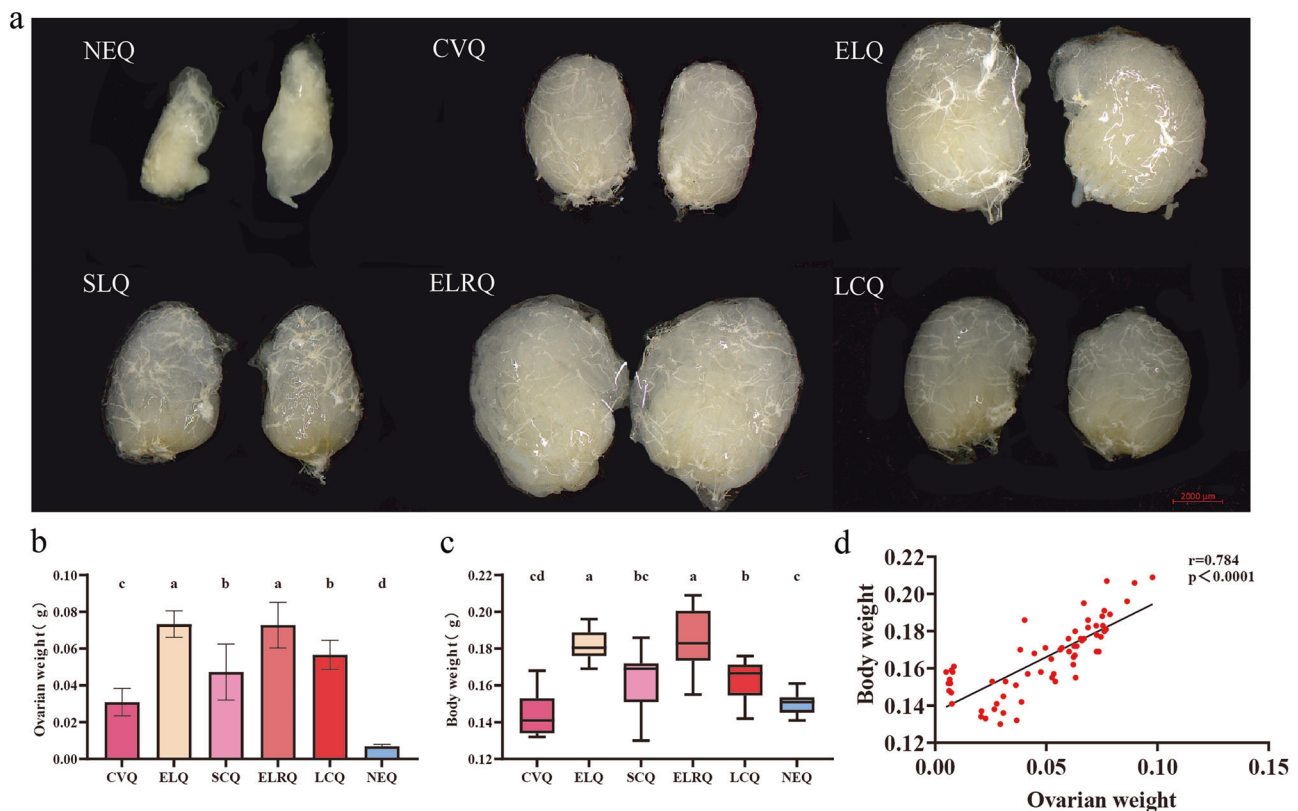


Fig. 1 | Effects of caged queen bees on ovary and body weight. a Microscopic image taken of the queen's ovary morphology, uniform use of 2000 µm scale. **b** Weight of the queens' ovaries. **c** Weight of the queen's body weight. **d** Correlation analysis of

the queen's ovary weight and body weight. (NEQ, $n = 10$. CVQ, $n = 11$. ERQ, $n = 10$. SCQ, $n = 11$. ELRQ, $n = 13$. LCQ, $n = 10$.)

Supplementary Table 1). These measurements were used to assess the development of the ovaries. NEQ ovaries weighed the least and CVQ ovaries weighed significantly less than mated queens (ELQ, SCQ, ELRQ, and LCQ). This suggests that the ovaries developed further after fertilization. A significant difference was observed between SCQ and ELQ, indicating that queen caging significantly inhibited ovarian development. However, there was no significant difference between SCQ and LCQ, suggesting that the duration of caging did not significantly affect ovarian development. Additionally, a significant difference was found between ELRQ and LCQ, but not between ELRQ and ELQ, indicating that the inhibition of ovarian development was lifted after re-laying, restoring the ovaries to the level of normal queen development. We also measured the queen's body weight (Fig. 1c and Supplementary Table 2), and analyzed its correlation with ovary weight, as depicted in Fig. 1d. Changes in body weight were generally consistent with changes in ovary weight, showing a strong correlation between the two.

Gut microbiota of the queens

The alpha diversity of queen's gut microbiota was assessed by shannon, simpson and chao1 (Fig. 2). The results showed that the different treatments had little effect on the alpha diversity of the midgut microbiota, and the structure of the midgut microbiota was relatively stable.

All amplicon sequence variants (ASVs) measured in this study were categorized at the phylum and genus levels. At the phylum level, the queen's midgut had the highest relative abundance of Proteobacteria, consistently the core phylum of the midgut. In contrast, the hindgut had a higher presence of Firmicutes, increasing from 43.39% to 73.86% in CVQ_H vs ELQ_H ($P = 0.03$). In contrast, the relative abundance of Proteobacteria decreased from 53.28% to 25.67% ($P = 0.04$), with the core phylum shifting from Proteobacteria to Firmicutes (Fig. 3a). Ovarian activation may have been associated with a change in the core phylum of the hindgut. At the

genus level, the dominant genus of bacteria in the midgut were *Brevundimonas* and *Ralstonia*, while *Lactobacillus* and *Bombella* were the dominant genus of bacteria in the hindgut. The microbiota structure in the midgut was relatively stable, whereas microbiota changes in the hindgut were more complex. Cluster analysis revealed that both ELQ and ELRQ had similar microbiota structures, suggesting that lifting the inhibition could somewhat restore the normal gut microbiota. The gut flora of NEQ was significantly different from that of the other groups, indicating that the gut microbiota undergoes a significant succession after the newly emerged queens enter the colony, even when ovarian activation and development is inhibited (Fig. 3b, c).

Tests of significance were conducted to determine the differences between dominant genera in the midgut and hindgut (Fig. 3d, e). *Ralstonia*, *Rhodococcus*, *Pseudoalteromonas*, and *Vibrio* displayed notable differences in the queen's midgut and hindgut, while *Lactobacillus* exhibited significant variations exclusively in the queen's hindgut. With regard to the queen's midgut, the relative abundances of *Rhodococcus*, *Pseudoalteromonas*, and *Vibrio* decreased during ovarian activation and developmental restriction, then increased to their original levels following the lifting of the inhibition. In the queen's hindgut, *Lactobacillus* had the highest relative abundance in CVQ_H, but its proportion decreased to 11.01% after 28 days of caging, and then increased to 39.92% ($P = 0.016$) following the lifting of the inhibition, approaching the 40.58% observed in ELQ_H. Conversely, *Ralstonia* showed an increasing trend in relative abundance as caging time progressed.

Using LEfSe analysis of variance, microorganisms with significant differences in the midgut and hindgut of queens from different caging treatments were screened (Fig. 4, LDA threshold of 3). Among highly abundant bacteria, Staphylococcales (from order to genus) was significantly enriched in CVQ_M, while Cbacilli (from order to genus) was significantly enriched in CVQ_H. Muribaculaceae (from family to genus) was

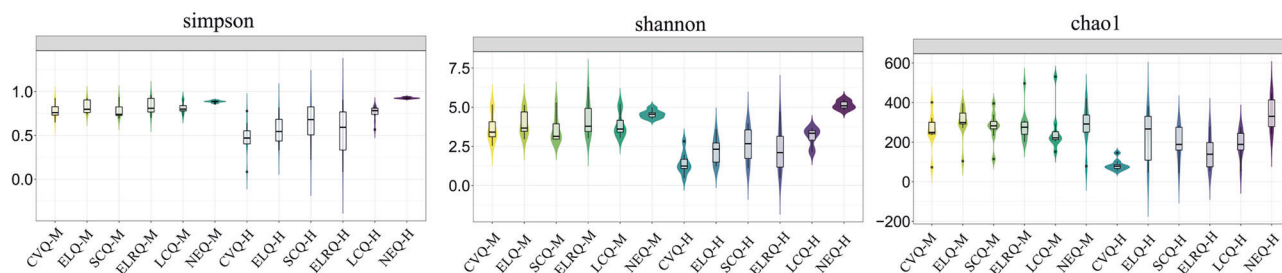


Fig. 2 | Alpha diversity of the queen's gut microbiome. M represents the midgut and H represents the hindgut. (CVQ, $n = 8$. ERQ, $n = 10$. SCQ, $n = 8$. ELRQ, $n = 10$. LCQ, $n = 8$. NEQ, $n = 6$).

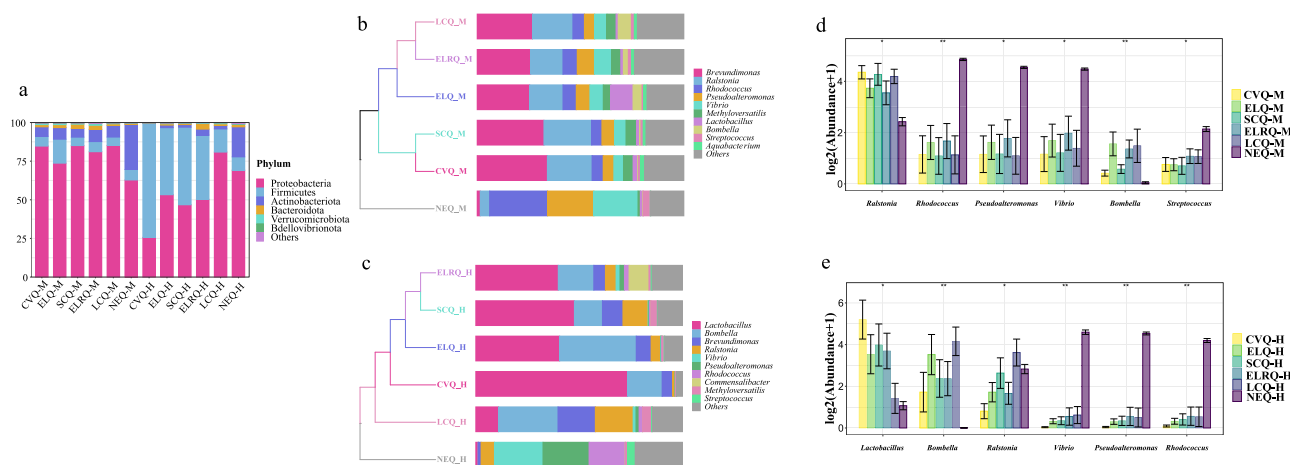


Fig. 3 | Community composition of the queen bee gut. a Horizontal community distribution of the middle and hindgut phyla. b Horizontal community distribution and clustering of midgut genera. c Horizontal community distribution and clustering of hindgut genera. d Differential genera in the midgut. e Differential genera in the hindgut.

significantly enriched in SCQ_M, whereas Apilactobacillus and Christensenellales (from order to family) were significantly enriched in SCQ_H. Additionally, Erwiniaceae (from family to genus) and Enterobacteriaceae (from family to genus) were enriched in LCQ_M, and Gammaproteobacteria (from order to species) were significantly enriched in LCQ_H. Furthermore, the hindgut of the queen exhibited a greater diversity of microorganisms, suggesting that hindgut bacteria are more diverse and more responsive to changes in the ovary. In addition, the LCQ group exhibited the most differential microbial composition, indicating that prolonged restriction of ovarian development has a significant impact on gut microbiota structure.

Ovarian metabolism of the queens

To further understand the changes in the ovary, we used ultra-high-performance liquid chromatography-tandem mass spectrometry (UHPLC-MS) to analyze ovarian metabolites. After processing, 950 metabolites were identified, with 907 annotated to public databases such as HMDB and Lipidmaps, and 581 annotated to KEGG (Supplementary Table 3). Metabolite differences between samples were determined by a supervised pattern recognition approach to maximize sample separation (Fig. 5a). The partial least squares discriminant analysis score plot explained 33.2% of the total variation among all groups, demonstrating clear separation and indicating that distinct regulatory constraints on ovarian activation and development can profoundly influence ovarian metabolite profiles. ELQ_O and ELRQ_O exhibited a relatively modest degree of separation, suggesting that ovarian metabolic processes may partially recover following the cessation of queen reproduction. The PLS-DA model validation indicated that the R^2 s for both the positive and negative ion modes were above Q2, suggesting a well-suited model for subsequent data analysis (Fig. 5b).

Metabolites of each ovary group were clustered and analyzed using a heatmap, and the distribution of differential metabolites in each group was visualized in the heatmap (Fig. 5c). Five differential metabolite subclusters were identified. Subcluster 1 showed high relative expression only in the CVQ_O group, suggesting a possible correlation with ovarian activation after virgin queen fertilization. Subcluster 2 exhibited low relative expression in ELQ_O and ELRQ_O. Subcluster 5 displayed high relative expression in ELQ_O and ELRQ_O, but was almost completely absent in CVQ_O, indicating that these metabolites may be associated with post-activation ovarian development. This suggests that lack of activation and developmental inhibition lead to alterations in metabolites in the ovary. Lack of ovarian activation in virgin queens has a more pronounced effect on the metabolites present in the ovary. However, metabolite levels have been observed to recover to some extent after ovarian suppression is lifted. Heat maps based on differential metabolites show significant clustering, thus confirming the reliability of the PLS-DA model in distinguishing queen bee ovarian metabolic phenotypes.

To further elucidate metabolites alterations associated with ovarian activation, development, and recovery, we compared ELQ_O with CVQ_O, SCQ_O with ELQ_O, and LCQ_O with ELRQ_O (Fig. 5d). Thirty eight differential metabolites were common to all groups, playing important roles in ovarian activation, development and recovery. Volcano diagrams were constructed based on the differences in metabolites between the two comparisons to demonstrate the specificity of metabolites (Fig. 5e, g, i). Clustered heatmaps and VIP bar charts were used to show the expression patterns of the top 30 metabolites in each differential group across samples and the P -values of the metabolites in the VIP and unidimensional statistics of multivariate statistical analyses, thus visualizing changes in the significance of the differential metabolites

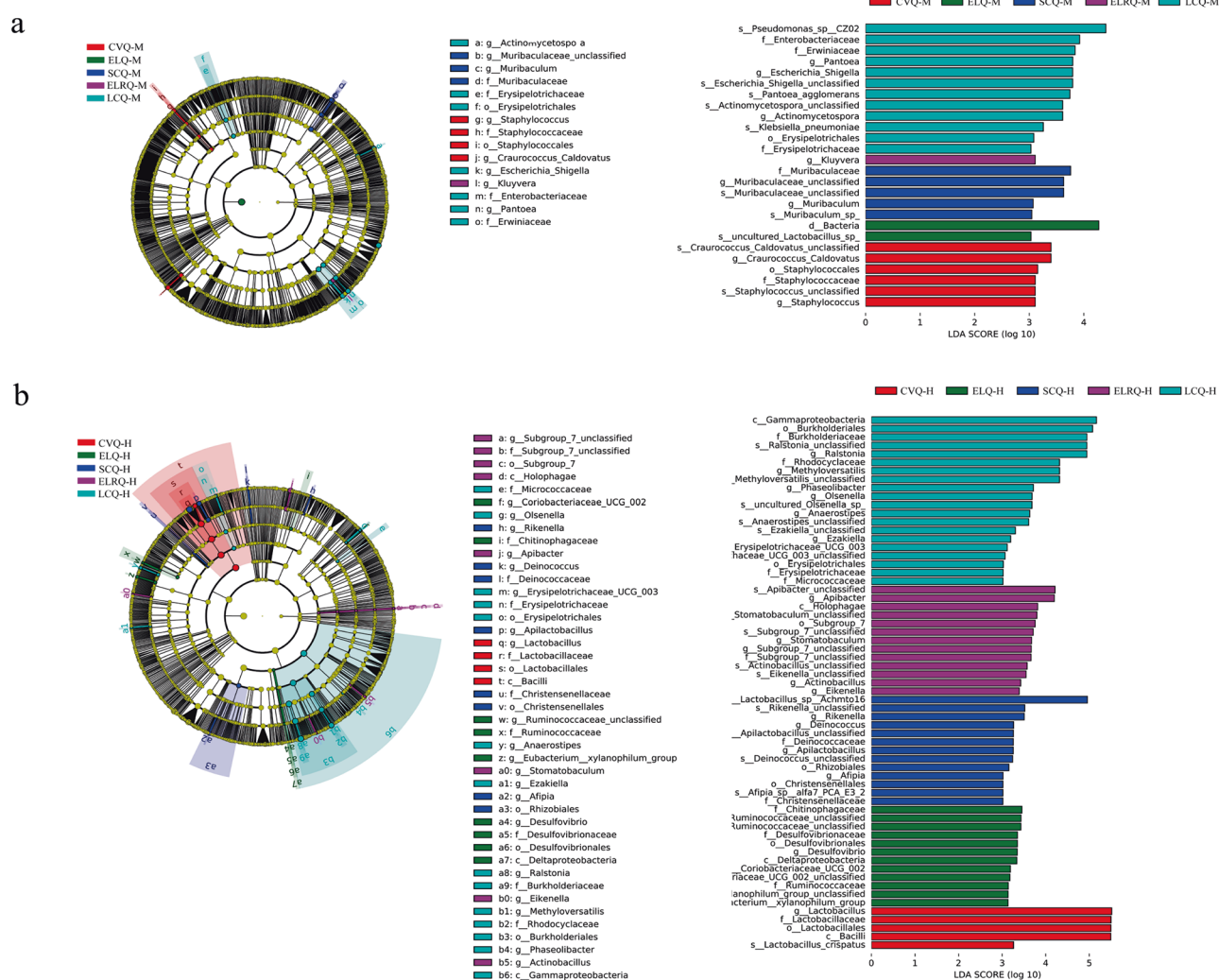


Fig. 4 | LEfSe (LDA effect size) analysis of the microbiota of the queen bee midgut and hindgut. a LEfSe analysis of the midgut. **b** LEfSe analysis of the hindgut.

and trends in their expression. Norepinephrine scored the highest during ovarian activation and was highly expressed in ELQ_O (Fig. 5f). NNAL-N-glucuronide scored the highest during ovarian development and was highly expressed in ELQ_O (Fig. 5h). Trinexapac-ethyl scored the highest during recovery and was highly expressed in ELRQ_O (Fig. 5j). These findings suggest that norepinephrine, NNAL-N-glucuronide, and trinexapac-ethyl may play significant roles in regulating ovarian activation, development, and recovery.

The mechanisms associated with ovarian activation, development, and recovery were revealed by KEGG pathway analysis (Fig. 6a–c). Purine metabolism exhibited the most significant impact ($P < 0.001$). Consequently, further research was conducted on the specific changes in metabolites involved in purine metabolism (Fig. 6d–i). Significant differences in the expression of six metabolites were found. Comparative analyses of these metabolites showed that adenosine 3',5'-diphosphate, dGDP, and ADP were significantly elevated, while xanthine, hypoxanthine, and inosine were decreased during ovarian activation, development, and recovery.

Based on the complete metabolite collection of the KEGG database, the metabolic network of changes occurring in the ovary was mapped using metabolomics data, allowing visualization of interactions in purine metabolic pathways (Fig. 6j). Combined with the differential expression of metabolites during ovarian activation, development, and recovery, the biosynthesis of guanine ribonucleotides, adenine ribonucleotides, and deoxyribonucleic acid was enhanced. Conversely, the degradation of guanine ribonucleotide and adenine ribonucleotide was inhibited.

Mechanisms of gut microbiota-gonadal axis interactions in queens

To explore the potential relationship between queen gut flora and ovarian metabolism, we selected the top 10 most abundant genera in the gut flora and the top 200 metabolites identified in the ovary. We evaluated the correlation between them, constructing separate correlation heatmaps for the midgut and hindgut flora with ovarian metabolites (Fig. 7). *Brevundimonas*, *Ralstonia*, *Rhodococcus*, *Vibrio*, *Bombella* and *Streptococcus* in the midgut were significantly correlated with the metabolic activities of the ovary (Fig. 7a and Supplementary Table 4). *Lactobacillus*, *Vibrio*, *Pseudoalteromonas*, *Rhodococcus*, *Commensalibacter* and *Bombilactobacillus* in the hindgut were significantly correlated with ovarian metabolites (Fig. 7b and Supplementary Table 5). Among them, *Brevundimonas*, *Vibrio*, *Bombella*, and *Lactobacillus* in the gut were strongly correlated with multiple ovarian metabolites. By analyzing the association between intestinal bacteria in the midgut and hindgut and purine metabolism, we found that *Bombella* and *Lactococcus* were significantly correlated with multiple metabolites in the purine metabolism pathway (Fig. 7c, d). These gut bacteria play an important role in regulating ovarian metabolism. Notably, metabolites such as dGDP (Fig. 6f) and ADP (Fig. 6i) in the purine pathway were significantly correlated with *Lactobacillus*, suggested that *Lactobacillus* in the hindgut may be involved in the regulation of metabolites in the ovary through the purine pathway.

Discussion

Our findings provide new insights into the reproductive biology of *Apis cerana* queens by highlighting the role of gut microbiota in ovarian

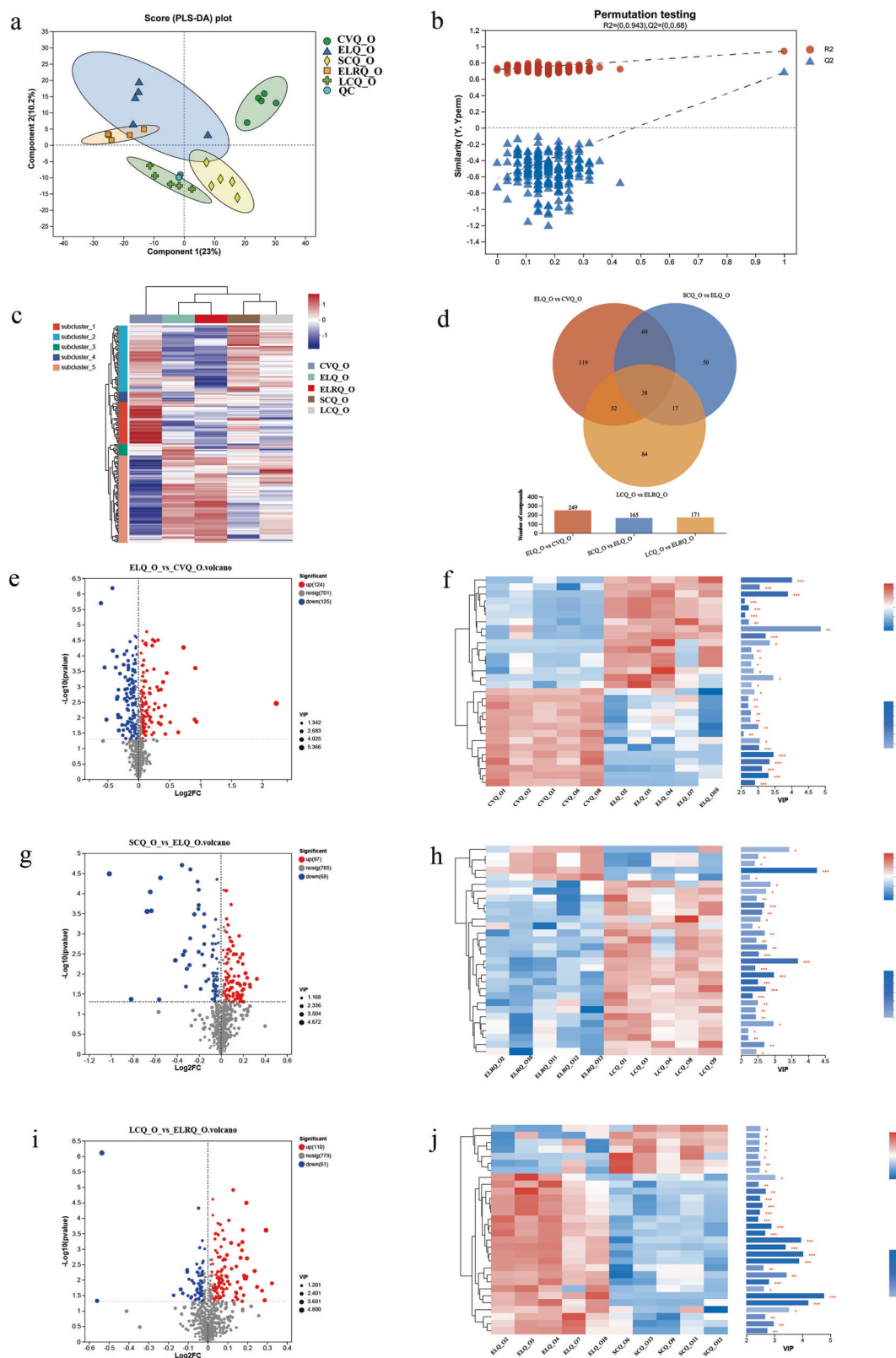


Fig. 5 | Metabolite changes in the ovary. a OPLS-DA analysis of ovarian metabolomics. **b** Validation of OPLS-DA analysis. **c** Sample and metabolite clustering analysis. **e** Volcano plot of ovarian differential metabolites in ELQ_O vs CVQ_O. **d** Venn diagram of multiple comparisons. **f** Clustering heatmaps and VIP bar graphs of ELQ_O vs CVQ_O. **g** Volcano plot of ovarian differential metabolites in SCQ_O vs ELQ_O. **h** Clustering heatmaps and VIP bar graphs of SCQ_O vs ELQ_O. **i** Volcano plot of ovarian differential metabolites in LCQ_O vs ELRQ_O. **j** Clustering heatmaps and VIP bar graphs of LCQ_O vs ELRQ_O. The length of the bar in the metabolite VIP bar graph indicates the contribution of the metabolite to the difference between the two groups. Bar colors indicate the significance of the metabolite difference between the two sample groups: * represents $P < 0.05$, ** represents $P < 0.01$, and *** represents $P < 0.001$.

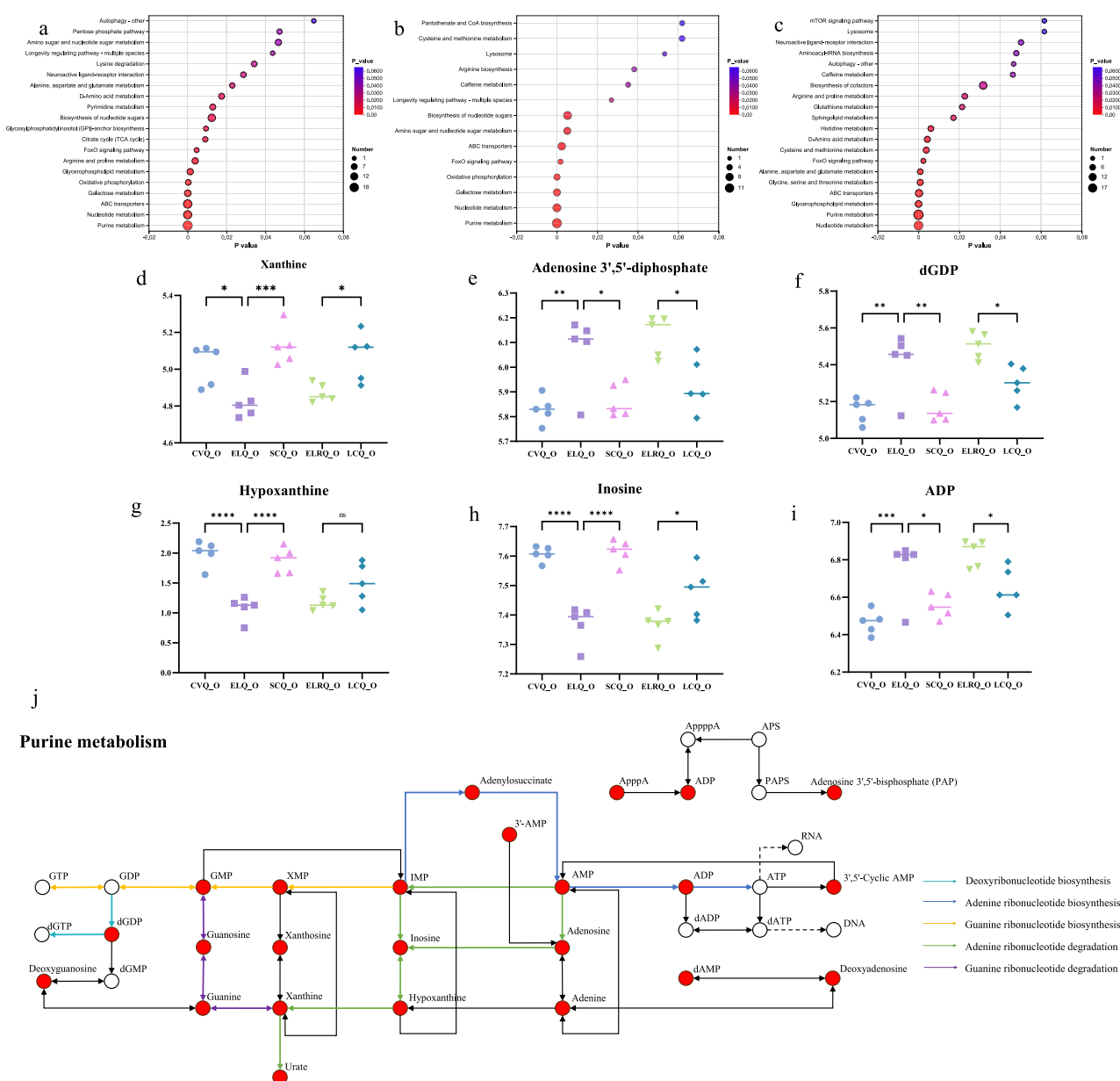


Fig. 6 | KEGG pathway enrichment analysis of differentially accumulated metabolites. a KEGG enrichment analysis (ELQ_O vs CVQ_O). **b** KEGG enrichment analysis (SCQ_O vs ELQ_O). **c** KEGG enrichment analysis (LCQ_O vs ELRQ_O). The horizontal coordinate is the enrichment significance p value, where a p value less than 0.05 is considered a significant enrichment term; the vertical coordinate is the KEGG pathway. The size of the bubbles in the graph represents the

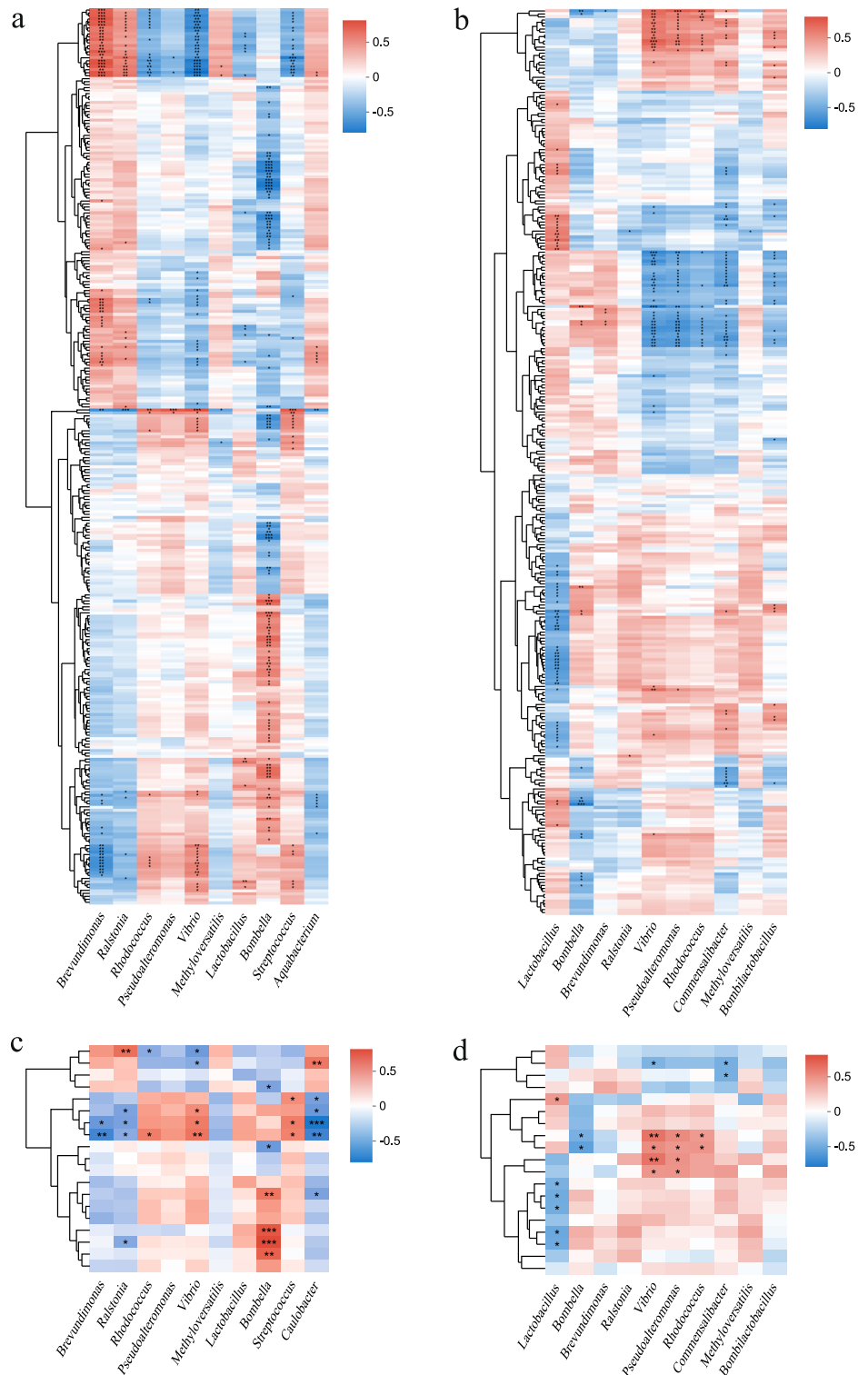
number of compounds enriched in the pathway in the metabolic set. **d–i** Changes in differential metabolites in purine metabolism, * represents $P < 0.05$, ** represents $P < 0.01$, *** represents $P < 0.001$, and **** represents $P < 0.0001$. **j** Response networks of differential metabolites in purine metabolic pathway. The red nodes are the differential metabolites in this study.

activation. While previous studies have primarily focused on *Apis mellifera*, our research reveals species-specific microbial influences on queen fertility in *A. cerana*. Given the distinct ecological adaptations and colony dynamics of *A. cerana*, its reproductive regulation may differ from that of *A. mellifera*, necessitating further investigation. This study advances our understanding by identifying gut microbiota as a previously underappreciated factor influencing *A. cerana* queen reproduction. These findings not only deepen our knowledge of microbial contributions to reproductive physiology but also suggest potential microbiota-based strategies to enhance queen fertility and colony health in *A. cerana* beekeeping.

With the economic value of honey production and their role as major pollinators for a wide range of food crops and plants, honey bees play a vital role in maintaining food security, ecological balance, and biodiversity. In

addition, the honey bee is a key model for research on social behaviors, learning and cognition, and gut microbiota^{42–44}. The morphology and weight of the ovaries of virgin queens are different from those of mated queens, and significant changes occur in the morphology of the ovaries and the distribution of cells in the ovarian ducts after the queen emerges from the hive⁴⁵. However, caged queens were unable to perform mate flight and failed to undergo ovarian activation⁴⁶. The most obvious visual evidence was a reduction in ovary weight by ~58% compared to mating-laying queens of the same age and a reduction in ovary size by ~35% compared to mating-restricted laying queens of the same age. Ovary size and weight were significantly reduced when the laying queen was caged, and when the queen was unable to lay eggs, the oocytes produced accumulated in the ovary. The excess oocytes may, in turn, inhibit the rate of oocyte production, mature

Fig. 7 | Correlation between gut bacteria and ovarian metabolites. **a** Correlation analysis of midgut dominant bacteria with ovarian metabolites. **b** Correlation analysis of hindgut dominant bacteria with ovarian metabolites. **c** Correlation analysis of midgut dominant bacteria with metabolites in purine metabolism. **d** Correlation analysis of hindgut dominant bacteria with metabolites in purine metabolism. Each grid in the figure represents the correlation between two attributes (ovarian metabolites and gut bacteria). The correlation coefficients in each square represent positive (red) and negative (blue) relationships. Statistically significant correlations are marked with asterisks (*). * represents $P < 0.05$, ** represents $P < 0.01$, *** represents $P < 0.001$.



oocytes degenerate in the late yolk stage, and programmed cell death occurs in the follicle, resulting in suppression of the queen's ovarian development^{47,48}. When the cage was removed, the queen resumed egg-laying, ovary inhibition was lifted, and ovary development continued, with a significant increase in ovary size and weight.

In egg-laying queen, the ovary occupies most of the abdominal cavity. Ovary weight has been studied as one of the physical criteria for assessing the reproductive potential of queens⁴⁹. Ovary size and fertility are usually positively correlated⁵⁰. However, beekeepers cannot assess ovarian

development by killing queens. In contrast, queen weight is intuitively easy to obtain, and the relationship between weight and fertility has been the research focus. The relationship between ovarian development and body weight is controversial. There is a positive correlation between ovarian development and body weight in *A. mellifera* and no correlation between queen ovarian development and body size in *Vespa analis*^{51–53}. The queen weight of *A. cerana* in our study was positively correlated with ovarian development. This reveals a correlation between fecundity and body size.

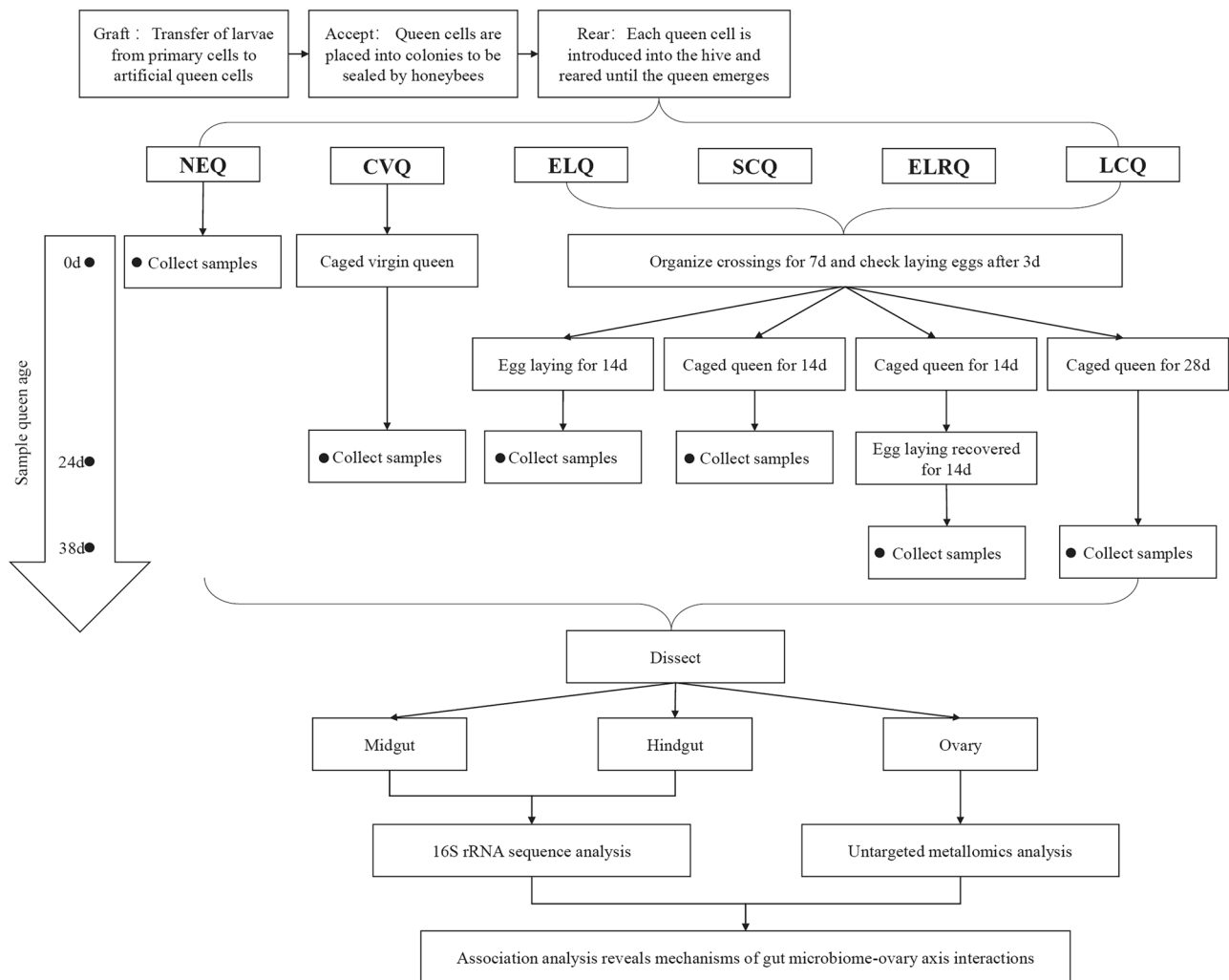


Fig. 8 | Schematic overview of study design. NEQ newly emerged queen, CVQ caged virgin queen, ELQ egg-laying queen, SCQ shortly-caged queen, ELRQ egg-laying recovered queen, LCQ longly-caged queen.

Significant differences were observed in microbiota structure between the midgut and hindgut of queen, with *Brevundimonas* and *Ralstonia* being the dominant genera in the midgut, while *Lactobacillus* and *Bombella* dominated in the hindgut. The microbial community in the hindgut exhibited greater volatility than in the midgut, and the hindgut gut microbiota composition exhibited two patterns: one dominated by *Lactobacillus* and the other by *Bombella*. In previous research, the genera *Brevundimonas*, *Ralstonia*, *Lactobacillus*, and *Bombella* were all identified in the queen gut, and were considered members of the core microbiome of the queen gut³³.

Compared to other older queens, the composition of the gut microbiota of newly emerged queens is significantly distinct. Following the queen's emergence, the gut microbiota undergoes a pronounced succession, with the appearance of certain bacteria at an early stage in the queen's life. Subsequently, the gut begins to be colonized by microorganisms obtained from the environment, enabling adaptation to the new environment. This succession may be primarily attributed to diet³⁴. This phenomenon occurs even in caged virgin queens as the queen's cage does not affect the queen's feeding by the worker bees⁵⁴.

Our results indicated that prolonged restriction of ovarian development was associated with a reduction in *Lactobacillus* and an elevation in *Ralstonia*. After disinhibition, there was an increase in the abundance of *Lactobacillus* and a decrease in the abundance of *Ralstonia*. *Lactobacillus* positively affected the ovaries, whereas *Ralstonia* may be negative for the ovaries. *Lactobacillus* is often considered a probiotic. The administration of *Lactobacillus* to rats with PCOS resulted in the normalization of ovarian morphology⁹. *Lactobacillus*

can scavenge free radicals from reproductive organs and maintain the normal histology of reproductive organs⁵⁵. There is a paucity of research investigating the impact of *Ralstonia* on ovarian development. Nevertheless, research has identified *Ralstonia* as a potential contributor to secondary infertility in patients⁵⁶. Furthermore, *Ralstonia solanacearum* is a plant pathogen that causes bacterial wilt, and male sterility occurs in affected individuals^{57,58}. We surmise that elevated levels of *Ralstonia* are responsible for ovarian atrophy during prolonged restriction of ovarian development. Conversely, elevated *Lactobacillus* levels are thought to drive the restoration of normal ovarian morphology after ovarian suppression is lifted.

During ovarian activation and development, metabolites undergo significant changes. We enriched differential metabolites for KEGG pathways and analyzed their correlation with the dominant genus of bacteria in the gut. Glycerophospholipid metabolism was significantly enriched during ovarian activation and development. Previous research has identified multiple effects of glycerophospholipid metabolism on follicular development. The intensities of the related metabolites in the pathway, phosphatidic acid (PA), phosphatidylcholine (PC), lysophosphatidylcholine (lysoPC) and lysophosphatidylethanolamine (lysoPE), correlated positively with the level of ovarian development and with the level of expression of the key enzyme in the pathway, glycerol-3-phosphate dehydrogenase 1-like (GPD1L). Knockdown of GPD1L induced mitochondrial dysfunction and granulosa cell apoptosis, lead to follicular atresia and impaired oocyte quality. Ovarian metabolic profiling in patients with biochemical premature ovarian insufficiency (bPOI) showed a significant reduction in PA, PC, lysoP, and lysoPE

in bPOI patients⁵⁹. In our study, these metabolites were significantly associated with *Brevundimonas* and *Vibrio*. Gut bacteria may influence the expression of PA, PC, lysoP, and lysoPE in the ovary by participating in glycerophospholipid metabolism and modulating ovarian activation.

We focused on purine metabolism signaling pathways, which showed the highest enrichment scores during ovarian activation, development, and recovery⁶⁰. Purines are abundant substrates in organisms and are vital raw materials for cell proliferation. Purinergic signalling may act as an intra-ovarian regulator of the balance between cell proliferation and death. Its activity may ultimately affect the function and fate of ovarian follicles^{61,62}. Our study indicated a strong correlation between *Lactobacillus* and various metabolites in the purine metabolic pathway. *Lactobacillus* may regulate the metabolic level of the ovary through the purine metabolic pathway and maintain the normal morphology of the ovary during ovarian activation. Purine metabolites, such as ATP/ADP, are central to cellular energy metabolism. In *Drosophila melanogaster*, gut microbiota depletion significantly reduce mitochondrial activity and ATP levels, impairing follicular cell development in the ovaries and decreasing reproductive capacity. However, supplementation with riboflavin, a mitochondrial coenzyme precursor that the host cannot synthesize de novo and must obtain from gut microbiota, restores mitochondrial function, ATP levels, and reproductive capacity. By providing mitochondrial coenzyme precursors, gut microbiota support the energy metabolism of the systemic and ovarian cells, thereby promoting oogenesis and ovarian activation⁶³. *Lactobacillus* species in gut microbiota enhance oocyte maturation and follicular development by reducing the accumulation of local ovarian purine metabolites (e.g., ATP), improving oxidative stress responses and mitochondrial function^{64–66}. Animal studies further demonstrate that *Lactobacillus* supplementation decreases the number of atretic follicles and increases the primordial follicle reserve⁶⁷. These findings strongly support for our results.

The initial step in the de novo synthesis of purine nucleotides is the conversion of hypoxanthine. The rate of purine metabolism is regulated by the negative feedback control of enzymes by hypoxanthine nucleotides. Many studies have been conducted on the function of hypoxanthine in various animals. These studies have demonstrated that hypoxanthine can inhibit meiotic reinitiation to some extent, maintain meiotic arrest in oocytes, effectively inhibit the onset of oocyte follicular maturation, and is a major inhibitor of oocyte maturation^{68–70}. We found that *Brevundimonas* and *Ralstonia* were positively correlated with hypoxanthine expression. Therefore, we hypothesize that a high abundance of *Ralstonia* in the intestine regulates the high expression of hypoxanthine through the purine metabolism pathway, causing ovarian atrophy. However, this hypothesis is based on correlational analyses, and current literature has not conclusively demonstrated a direct negative impact of *Ralstonia* on ovarian function. Whether *Ralstonia* or its metabolites disrupt ovarian homeostasis requires further experimental validation.

Our findings suggest that microbiota modulation may serve as a promising strategy to enhance bee reproduction, with potential applications in apiculture. One possible approach is the supplementation of probiotics containing beneficial microbial strains that support queen fertility and colony health. Additionally, dietary interventions, such as pollen substitutes enriched with key microbial species, could help maintain a stable and functionally beneficial gut microbiota in managed colonies. These strategies may improve reproductive success, enhance resistance to environmental stressors, and promote overall colony stability. However, before implementing microbiota-based interventions in beekeeping, factors such as strain specificity, scalability, cost-effectiveness, and potential ecological impacts must be carefully evaluated. Future research should explore the long-term effects of microbiota modulation on queen longevity, brood production, and colony performance to determine its feasibility as a sustainable beekeeping practice.

This study provides scientific evidence supporting the existence and mechanistic basis of the gut microbiota-gonadal axis through systematic investigation of the relationship between intestinal microbiota and ovarian activation. However, several limitations warrant careful consideration. First, while our correlation-based analysis generated multiple hypotheses, the

current lack of supporting literature leaves some propositions insufficiently substantiated, necessitating deeper mechanistic investigations in subsequent research. Second, although the experimental design rigorously controlled for variables such as age and rearing environment, complete elimination of external confounding factors remained unattainable. Notably, prolonged confinement may induce chronic stress in queen bees, potentially altering gut microbiota composition. Furthermore, dietary modifications during captivity could modify nutritional substrates and environmental conditions essential for microbial growth, deviating from natural nutritional patterns. Future investigations should prioritize establishing causal relationships between gut microbiota dynamics and ovarian activation mechanisms.

In summary, ovarian morphology, weight, and metabolites change markedly during the queen ovary's activation, development, and recovery, and these changes are strongly correlated with the gut microbiota. Our study supports the existence of a gut microbiota-gonadal axis and finds that the mechanisms of action are complex. On the one hand, the presence of specific bacteria in the gut regulates a wide range of metabolites in the ovary. On the other hand, a wide range of gut microbes synergistically regulate specific metabolites in the ovary. We provide several potential mechanisms of interactions. These findings offer new insights into the gut microbiota-gonadal axis. It also provides a theoretical basis for gut microbiota to promote reproductive health in honey bees.

Methods

Queen rearing and sample collection

The experiment was conducted from February through April 2023, and the *A. cerana* colonies used in this study were kept at the experimental apiary of the Institute of Zoology, Guangdong Academy of Sciences, Guangzhou, China (23°504400 N, 113°1701700 E). To strictly control variables such as age and growth environment, queens were reared according to the standard methods^{71,72}. Briefly, 1-day-old worker larvae were individually grafted from a donor colony to handmade wax queen cups on the same day. Then the breeding frames with queen cups were inserted into a rearing colony that was deprived of the queen and all natural queen cups in advance. Ten days later, most of the queen cups were distributed to the recipient colonies, which were prepared following the same standards: healthy, equal colony strength, capped brood area, and food availability, and also had the old queens taken out and natural queen cups destroyed. The remaining queen cups were brought to the laboratory and kept in an incubator (34.5 °C, 70% RH) until emergence; once they emerged, the queens were collected as the newly emerged queens (NEQ, $n = 10$). All the queens kept in the receipt colonies successfully emerged; once they emerged, eleven of them were randomly selected and caged until being sampled as the caged virgin queens (CVQ, $n = 11$). The left virgin queens were freely mated and their egg-laying was examined 10 days after emergence. Those without egg laying were discarded and the remaining egg-laying queens were further divided into four groups: (1) egg-laying queens (ELQ, $n = 10$): the queens were let lay eggs for 14 days, then sampled; (2) shortly-caged queens (SCQ, $n = 11$): the queens were caged for 14 days until sampling; (3) egg-laying recovered queens (ELRQ, $n = 13$): the queens were first caged for 14 days, then released to lay eggs for 14 days until sampling; (4) longly-caged queen (LCQ, $n = 10$): the queens were always caged for nearly 1 month until sampling. The details on the treatment and sampling of queens are shown in Fig. 8. All queen samples were stored at -80°C for subsequent experiments.

Anatomy of queen bees

Standard methods for honey bee dissection were used⁷³. All experiments were conducted in a sterile environment and all tools were sterilized prior to use. The sample queen was first weighed on a balance and the data was recorded. The queen sample body was thoroughly washed in 75% alcohol and phosphate buffer saline (PBS), and then fixed on a wax disk using an insect needle. The dorsal plate was incised in a V-shape from the caudal end of the abdomen sequentially, and the open abdominal cavity was secured with three pairs of insect needles. The incised dorsal plate was then separated and secured to the wax discs on both sides of the queen's body. The pair of

ovaries and intact gut were then removed with forceps. The queen's ovaries were photographed using a microscope. The centrifuge tubes were weighed in advance, and the ovaries were placed in the centrifuge tubes and weighed on a balance. The weight of the sample tubes was subtracted to arrive at the net weight of the ovaries and recorded. Meanwhile, the midgut and hindgut were separated from the intact gut and placed in separate sample centrifuge tubes. The samples were snap-frozen with liquid nitrogen and stored in a -80°C refrigerator.

Gut microbiota extraction and sequencing analysis

Queen intestinal samples were homogenized using the bead mill method. The lysed samples were subjected to DNA extraction using the Insect DNA Kit (Do926-02; Omega, USA) according to the manufacturer's instructions. The extracted DNA was measured and evaluated using the NanoMicro-Drop 2000 (Thermo Scientific, Wilmington, USA) and 2% agarose gel electrophoresis to measure and assess the concentration and quality.

The extracted intestinal bacterial DNA was amplified by PCR using universal primers 341F (5'-CCTACGGGNGGCWGCAG-3') and 805 R (5'-GACTACHVGGGTATCTAATCC-3'), which are highly conserved in the 16S rRNA V3 to V4 region. The selection of the V3-V4 region of the 16S rRNA as the target sequencing area is due to its moderate length, high degree of variability, strong primer universality, and its ability to effectively balance the limitations of sequencing technology with the need for high taxonomic resolution. The amplification system consisted of 12.5 μL of Phusion Hot Start Flex 2X Master Mix, 2.5 μL of Forward Primer, 2.5 μL of Reverse Primer, and 50 ng of DNA template, with ddH₂O added to get a final volume of 25 μL . Amplification was performed under the following conditions: 35 cycles of 98°C for 30 s, 98°C for 10 s, 54°C for 30 s, and 72°C for 45 s, followed by a final extension at 72°C for 10 min and an indefinite hold at 4°C . PCR products were purified using AMPure XT beads (Beckman Coulter Genomics, Danvers, MA, USA) and quantified using Qubit (Invitrogen, USA). The purified PCR products were evaluated using Agilent 2100 Bioanalyzer (Agilent, USA) and Illumina library quantification kits (Kapa Biosciences, Woburn, MA, USA). Qualified libraries should have a concentration of 2 nM or more. After gradient dilution of each qualified up-sequencing library (Index sequences were not reproducible), the libraries were mixed in the appropriate ratio according to the required sequencing volume and denatured by NaOH to single-stranded for sequencing. The sequencing was performed using the NovaSeq 6000 sequencer from LC-Bio Technologies (Hangzhou) Co., Ltd. (<https://www.omicstudio.cn/tool/1>) with 2×250 bp paired-end reads using the NovaSeq 6000 SP Reagent Kit (500 cycles). Samples were demultiplexed for the paired-end data obtained by sequencing based on the barcode information and remove the splice and barcode sequences. Data splicing and filtering involved removing primer sequences and balanced base sequences from RawData, merging each pair of paired-end reads into one longer tag according to the overlap region splicing and performing quality scanning of sequencing reads by the window method. Perform a window method quality scan on sequencing READs, with a default scanning window of 100 bp, and truncate the READ from the start of the window to the 3' termination when the average quality value within the window is less than 20. Sequences with a length of less than 100 bp after truncation, sequences with more than 5% N (indeterminate bases), and chimeric sequences were removed. Length filtering and denoising were performed by qiime dada2 denoise-paired tuning DADA2 (<https://qiime2.org/>). To obtain representative sequences with single-nucleotide resolution, we employed the DADA2 (Divisive Amplicon Denoising Algorithm) method. Processes such as "dereplication" (analogous to clustering based on 100% similarity) were performed to enhance data accuracy and species resolution, ultimately generating precise representative sequences. The fundamental principle of DADA2 involves noise reduction, followed by using the denoised sequences to construct the final feature list of ASVs and their characteristic sequences for downstream diversity analysis, species classification annotation, and differential analysis.

Before conducting α -diversity and β -diversity analyses, sequence counts for each sample were standardized using a rarefaction approach,

which reduces the sequence counts of all samples to the level of the sample with the fewest sequences. For species composition analysis, a relative abundance normalization method was applied, with the calculation formula being: count of X bacterial group/total count.

The SILVA (Release 138, <https://www.arbsilva.de/documentation/release138/>) database was used to annotate species with the NT-16S database, and the abundance of each species in each sample was counted. The confidence threshold for annotation was set at 0.7.

Untargeted metabolomics analysis of ovarian

Fifty milligrams of the ovarian sample were weighed into a 2 mL centrifuge tube and 6 mm diameter grinding beads were added. An extract (400 μL ; methanol: acetonitrile = 1:1, v/v) containing four internal standards (L-2-chlorophenylalanine, etc.) was added. A low-temperature tissue grinder was used for 6 min (-10°C , 50 Hz). Low-temperature ultrasonic extraction was performed for 30 min (5°C , 40KHz). Samples were placed at -20°C for 30 min, centrifuged for 15 min ($13,000 \times g$, 4°C), and the supernatant was transferred to injection vials with internal cannulae for analysis. Additionally, 20 μL of supernatant was removed from each sample, mixed, and used as a quality control (QC) sample.

Chromatographic conditions were as follows: the column was an ACQUITY UPLC HSS T3 (100 mm \times 2.1 mm i.d., 1.8 μm ; Waters Corporation, Milford, USA); mobile phase A was 95% water + 5% acetonitrile (containing 0.1% formic acid); mobile phase B was 47.5% acetonitrile + 47.5% isopropanol + 5% water (containing 0.1% formic acid), and the injection volume was 3 μL . The column temperature was 40°C .

Mass spectrometry conditions were as follows: samples were subjected to electro spray ionization, and mass spectra were acquired in positive and negative ion scanning modes. The scan range was 70–1050 m/z; the sheath gas flow rate was 50 arb; the auxiliary gas flow rate was 13 arb; the heating temperature was 425°C ; the capillary temperature was 325°C ; the spray voltage (+) was 3500 V; the spray voltage (–) was -3500 V; and the S-lens voltage was 50.

Quality control (QC) samples are prepared by mixing the extracts of all samples in equal volume. Every QC has the same volume as the sample and is handled and detected in the same way as the analyzed sample. During instrumental analysis, one QC sample is inserted every 5–15 analyzed samples to check the stability of the detection process.

Statistical analysis

Statistical analysis was performed by using Graph Pad Prism version 9.5.0. The Kruskal-Wallis test was used for all non-parametric tests, and the one-way analysis of variance (ANOVA) test was used for all parametric tests. $P < 0.05$ was considered as statistically significant. Spearman was used to analyze the correlation between major bacterial communities and these detected metabolites.

Data availability

Raw data for 16S rRNA sequencing have been deposited in the NCBI database under BioProject PRJNA1147442. Any additional information required to re-analyze the data reported in this work is available from the lead contact upon request.

Code availability

The code used in this study is available upon request.

Received: 5 August 2024; Accepted: 8 May 2025;

Published online: 07 June 2025

References

1. Ashonibare, V. J., Akorede, B. A., Ashonibare, P. J., Akhigbe, T. M. & Akhigbe, R. E. Gut microbiota-gonadal axis: the impact of gut microbiota on reproductive functions. *Front. Immunol.* **15**, 1346035 (2024).
2. Argaw-Denboba, A. et al. Paternal microbiome perturbations impact offspring fitness. *Nature* **629**, 652–659 (2024).

3. Fu, Y. et al. Landscape of the gut mycobiome dynamics during pregnancy and its relationship with host metabolism and pregnancy health. *Gut* **73**, 1302–1312 (2024).
4. Xu, B. et al. Multi-omics analysis reveals gut microbiota-ovary axis contributed to the follicular development difference between Meishan and Landrace × Yorkshire sows. *J. Anim. Sci. Biotechnol.* **14**, 68 (2023).
5. Qi, X., Yun, C., Pang, Y. & Qiao, J. The impact of the gut microbiota on the reproductive and metabolic endocrine system. *Gut Microbes* **13**, 1894070 (2021).
6. Elgart, M. et al. Impact of gut microbiota on the fly's germ line. *Nat. Commun.* **7**, 11280 (2016).
7. Han, S., Shannahan, S. & Pellish, R. Fecal microbiota transplant: treatment options for clostridium difficile infection in the intensive care unit. *J. Intensive Care Med.* **31**, 577–586 (2016).
8. Wu, J. et al. Association between premature ovarian insufficiency and gut microbiota. *BMC Pregnancy Childbirth* **21**, 418 (2021).
9. Guo, Y. et al. Association between polycystic ovary syndrome and gut microbiota. *PLoS ONE* **11**, e0153196 (2016).
10. Xu, L. et al. Fecal microbiota transplantation from young donor mice improves ovarian function in aged mice. *J. Genet. Genom.* **49**, 1042–1052 (2022).
11. Antwis, R. E., Edwards, K. L., Unwin, B., Walker, S. L. & Shultz, S. Rare gut microbiota associated with breeding success, hormone metabolites and ovarian cycle phase in the critically endangered eastern black rhino. *Microbiome* **7**, 27 (2019).
12. Tarpy, D. R., Nielsen, R. & Nielsen, D. I. A scientific note on the revised estimates of effective paternity frequency in *Apis*. *Insect Soc.* **51**, 203–204 (2004).
13. Woyke, J. Natural and artificial insemination of queen honeybees. *Bee World* **43**, 21–25 (1962).
14. Tanaka, E. D. & Hartfelder, K. The initial stages of oogenesis and their relation to differential fertility in the honey bee (*Apis mellifera*) castes. *Arthropod Struct. Dev.* **33**, 431–442 (2004).
15. Oxley, P. R. & Oldroyd, B. P. The genetic architecture of honeybee breeding. in *Advances in Insect Physiology* Vol. 39 (ed. Simpson, S. J.) 83–118, Ch. 3 (Academic Press, 2010).
16. Chen, X. et al. Integration of lncRNA–miRNA–mRNA reveals novel insights into oviposition regulation in honey bees. *PeerJ* **5**, e3881 (2017).
17. Döke, M. A., Frazier, M. & Grozinger, C. M. Overwintering honey bees: biology and management. *Curr. Opin. Insect Sci.* **10**, 185–193 (2015).
18. Shehata, S. M., Townsend, G. F. & Shuel, R. W. Seasonal physiological changes in queen and worker honeybees. *J. Apic. Res.* **20**, 69–78 (1981).
19. Büchler, R. et al. Summer brood interruption as integrated management strategy for effective Varroa control in Europe. *J. Apic. Res.* **59**, 764–773 (2020).
20. Gregorc, A., Alburaki, M., Werle, C., Knight, P. R. & Adamczyk, J. Brood removal or queen caging combined with oxalic acid treatment to control varroa mites (*Varroa destructor*) in honey bee colonies (*Apis mellifera*). *Apidologie* **48**, 821–832 (2017).
21. Tarpy, D. R., Keller, J. J., Caren, J. R. & Delaney, D. A. Assessing the mating ‘Health’ of commercial honey bee queens. *J. Econ. Entomol.* **105**, 20–25 (2012).
22. Thompson, G. J., Yockey, H., Lim, J. & Oldroyd, B. P. Experimental manipulation of ovary activation and gene expression in honey bee (*Apis mellifera*) queens and workers: testing hypotheses of reproductive regulation. *J. Exp. Zool. A Ecol. Genet. Physiol.* **307A**, 600–610 (2007).
23. Niu, D. et al. Transcriptome comparison between inactivated and activated ovaries of the honey bee *Apis mellifera* L. *Insect Mol. Biol.* **23**, 668–681 (2014).
24. Statello, L., Guo, C.-J., Chen, L.-L. & Huarte, M. Gene regulation by long non-coding RNAs and its biological functions. *Nat. Rev. Mol. Cell Biol.* **22**, 96–118 (2021).
25. Macedo, L. M. F. et al. MicroRNA signatures characterizing caste-independent ovarian activity in queen and worker honeybees (*Apis mellifera* L.). *Insect Mol. Biol.* **25**, 216–226 (2016).
26. Chen, X., Shi, W. & Chen, C. Differential circular RNAs expression in ovary during oviposition in honey bees. *Genomics* **111**, 598–606 (2019).
27. Zhong, S., Pan, L., Wang, Z. & Zeng, Z. Revealing changes in ovarian and hemolymphatic metabolites using widely targeted metabolomics between newly emerged and laying queens of honeybee (*Apis mellifera*). *Insects* **15**, 263 (2024).
28. Kwong, W. K. & Moran, N. A. Gut microbial communities of social bees. *Nat. Rev. Microbiol.* **14**, 374–384 (2016).
29. Tarpy, D. R., Mattila, H. R. & Newton, I. L. G. Development of the honey bee gut microbiome throughout the queen-rearing process. *Appl. Environ. Microbiol.* **81**, 3182–3191 (2015).
30. Vojvodic, S., Rehan, S. M. & Anderson, K. E. Microbial gut diversity of Africanized and European honey bee larval instars. *PLoS ONE* **8**, e72106 (2013).
31. Corby-Harris, V. et al. Origin and effect of Alpha 2.2 *Acetobacteraceae* in honey bee larvae and description of *Parasaccharibacter apium* gen. nov., sp. nov. *Appl. Environ. Microbiol.* **80**, 7460–7472 (2014).
32. Yun, J.-H., Lee, J.-Y., Hyun, D.-W., Jung, M.-J. & Bae, J.-W. *Bombella apis* sp. nov., an acetic acid bacterium isolated from the midgut of a honey bee. *Int. J. Syst. Evol. Microbiol.* **67**, 2184–2188 (2017).
33. Yang, J. et al. The dominating role of genetic background in shaping gut microbiota of honeybee queen over environmental factors. *Front. Microbiol.* **12**, 722901 (2021).
34. Anderson, K. E. et al. The queen's gut refines with age: longevity phenotypes in a social insect model. *Microbiome* **6**, 108 (2018).
35. Bosmans, L. et al. Hibernation leads to altered gut communities in bumblebee queens (*Bombus terrestris*). *Insects* **9**, 188 (2018).
36. Wang, L. et al. Dynamic changes of gut microbial communities of bumble bee queens through important life stages. *mSystems* **4**, e00631–19 (2019).
37. Powell, J. E., Eiri, D., Moran, N. A. & Rangel, J. Modulation of the honey bee queen microbiota: effects of early social contact. *PLoS ONE* **13**, e0200527 (2018).
38. Li, W.-L. et al. Gut microbiota-driven regulation of queen bee ovarian metabolism. *Microbiol. Spectr.* **11**, e02145–23 (2023).
39. Oldroyd, B. P. & Wongsiri, S. *Asian Honey Bees: Biology, Conservation, and Human Interactions* (Harvard University Press, 2006).
40. Ruttner, F., Woyke, J. & Koeniger, N. Reproduction in *Apis cerana* 2. Reproductive organs and natural insemination. *J. Apic. Res.* **12**, 21–34 (1973).
41. Ruttner, F., Woyke, J. & Koeniger, N. Reproduction in *Apis cerana* 1. mating behaviour. *J. Apic. Res.* **11**, 141–146 (1972).
42. Zheng, H., Steele, M. I., Leonard, S. P., Motta, E. V. S. & Moran, N. A. Honey bees as models for gut microbiota research. *Lab Anim.* **47**, 317–325 (2018).
43. Srinivasan, M. V. Honey bees as a model for vision, perception, and cognition. *Annu. Rev. Entomol.* **55**, 267–284 (2010).
44. Sokolowski, M. B. Social interactions in “Simple” model systems. *Neuron* **65**, 780–794 (2010).
45. Patricio, K. & Cruz-Landim, C. Mating influence in the ovary differentiation in adult queens of *Apis mellifera* L. (Hymenoptera, Apidae). *Braz. J. Biol.* **62**, 641–649 (2002).
46. Melo, G. A. R., Buschini, M. L. T. & Campos, L. A. O. Ovarian activation in *Melipona quadrifasciata* queens triggered by mating plug stimulation (Hymenoptera, Apidae). *Apidologie* **32**, 355–361 (2001).
47. Aamidor, S. E. et al. Reproductive plasticity and oogenesis in the queen honey bee (*Apis mellifera*). *J. Insect Physiol.* **136**, 104347 (2022).
48. Eppig, J. J., Wigglesworth, K. & Pendola, F. L. The mammalian oocyte orchestrates the rate of ovarian follicular development. *Proc. Natl. Acad. Sci. USA* **99**, 2890–2894 (2002).

49. Kahya, Y., Gençer, H. V. & Woyke, J. Weight at emergence of honey bee (*Apis mellifera caucasica*) queens and its effect on live weights at the pre and post mating periods. *J. Apic. Res.* **47**, 118–125 (2008).
50. Tarpy, D. R., Hatch, S. & Fletcher, D. J. C. The influence of queen age and quality during queen replacement in honeybee colonies. *Anim. Behav.* **59**, 97–101 (2000).
51. Zhu, K. et al. Plant microRNAs in larval food regulate honeybee caste development. *PLOS Genet.* **13**, e1006946 (2017).
52. Kaftanoglu, O., Linksvayer, T. A. & Page, R. E. Jr Rearing honey bees (*Apis mellifera* L.) in vitro: effects of feeding intervals on survival and development. *J. Apic. Res.* **49**, 311–317 (2010).
53. Kudô, K. et al. Mating and post-hibernation ovarian development in stylopized and non-stylopized queens of the hornet *Vespa analis* (Hymenoptera Vespidae). *Ethol. Ecol. Evol.* **36**, 86–95 (2024).
54. Vojvodic, S. et al. The transcriptomic and evolutionary signature of social interactions regulating honey bee caste development. *Ecol. Evol.* **5**, 4795–4807 (2015).
55. Amdekar, S. & Singh, V. *Lactobacillus acidophilus* maintained oxidative stress from reproductive organs in collagen-induced arthritic rats. *J. Hum. Reprod. Sci.* **9**, 41 (2016).
56. Carrell, D. T., Emery, B. R. & Hamilton, B. Seminal infection with *Ralstonia picketti* and cytolysosomal spermophagy in a previously fertile man. *Fertil. Steril.* **79**, 1665–1667 (2003).
57. Wai, K. P. P., Lee, J., Mo, H.-S. & Kim, B.-S. Sources of resistance to bacterial wilt and restorer-of-fertility genotype for cytoplasmic male sterility in *Capsicum* pepper. *Hortic. Environ. Biotechnol.* **54**, 266–271 (2013).
58. Andino, M. et al. Potato introgressive hybridisation breeding for bacterial wilt resistance using solanum commersonii dun. as donor: genetic and agronomic characterisation of a backcross 3 progeny. *Potato Res.* **65**, 119–136 (2022).
59. Zhao, X. et al. P-637 pseudo-targeted metabolomics of follicular fluid reveals ovarian GPD1L-mediated glycerophospholipid metabolism dysfunction in patients with biochemical premature ovarian insufficiency. *Hum. Reprod.* **38**, dead093.965 (2023).
60. Liu, J. et al. Targeting purine metabolism in ovarian cancer. *J. Ovarian Res.* **15**, 93 (2022).
61. Vázquez-Cuevas, F. G., Zárate-Díaz, E. P., Garay, E. & Arellano, R. O. Functional expression and intracellular signaling of UTP-sensitive P2Y receptors in theca-interstitial cells. *Reprod. Biol. Endocrinol.* **8**, 88 (2010).
62. Martínez-Ramírez, A. S. & Vázquez-Cuevas, F. G. Purinergic signaling in the ovary. *Mol. Reprod. Dev.* **82**, 839–848 (2015).
63. Gnainsky, Y. et al. Systemic regulation of host energy and oogenesis by microbiome-derived mitochondrial coenzymes. *Cell Rep.* **34**, 108583 (2021).
64. Li, M. et al. *Lactiplantibacillus plantarum* enables blood urate control in mice through degradation of nucleosides in gastrointestinal tract. *Microbiome* **11**, 153 (2023).
65. Liu, X. et al. Mechanisms of probiotic modulation of ovarian sex hormone production and metabolism: a review. *Food Funct.* **15**, 2860–2878 (2024).
66. Gao, M. et al. Characterization of metabolic patterns in porcine cumulus cells during meiotic maturation. *Theriogenology* **220**, 56–69 (2024).
67. Shooshtar, M. J. P., Ramezani, M. & Andoohjerdi, R. B. Effect of *Lactobacillus plantarum* on folliculogenesis in deep frying oil-fed rats. *Reprod. Toxicol.* **115**, 157–162 (2023).
68. Downs, S. M., Coleman, D. L., Ward-Bailey, P. F. & Eppig, J. J. Hypoxanthine is the principal inhibitor of murine oocyte maturation in a low molecular weight fraction of porcine follicular fluid. *Proc. Natl. Acad. Sci. USA* **82**, 454–458 (1985).
69. Eppig, J. J. & Downs, S. M. The effect of hypoxanthine on mouse oocyte growth and development in vitro: Maintenance of meiotic arrest and gonadotropin-induced oocyte maturation. *Dev. Biol.* **119**, 313–321 (1987).
70. Wang, J. et al. Melatonin alleviates the suppressive effect of hypoxanthine on oocyte nuclear maturation and restores meiosis via the melatonin receptor 1 (MT1)-mediated pathway. *Front. Cell Dev. Biol.* **9**, 648148 (2021).
71. Abrol, D. P., Bhagat, R. M. & Sharma, D. Mass rearing of *Apis cerana* F. queen. *J. Asia-Pac. Entomol.* **8**, 309–317 (2005).
72. Büchler, R. et al. Standard methods for rearing and selection of *Apis mellifera* queens 2.0. *J. Apic. Res.* **0**, 1–57 (2024).
73. Carreck, N. L. et al. Standard methods for *Apis mellifera* anatomy and dissection. *J. Apic. Res.* **52**, 1–40 (2013).

Acknowledgements

We thank Yuqiang Wang and Yang Gao for their technical assistance for queen rearing and sampling. This work was supported by the GDAS' Project of Science and Technology Development (Grant numbers 2022GDASZH-2022010102), the National Natural Science Foundation of China (Grant number 32000347, 32260863), the Seed Industry Revitalization Action of the Department of Agriculture and Rural Affairs of Guangdong Province (Grant number 2024-XPY-00-014), the Guangzhou Science and Technology Plan Project (Grant number 202103000009), and the Talent Project of Guangdong Institute of Applied Biological Resources (Grant number GIABR-gjrc201702).

Author contributions

R.H., S.H., J.G. and W.L. designed the study. C.Z., Y.P. and W.L. collected and processed samples. Y.P., M.F.R. and W.W. conducted the laboratory analyses. C.Z., Y.P., W.L. and Y.Z. performed the data processes. C.Z., W.L., Y.C., J.G., S.H. and R.H. wrote the manuscript. All authors edited and approved the final manuscript.

Competing interests

The authors declare no competing interests.

Additional information

Supplementary information The online version contains supplementary material available at <https://doi.org/10.1038/s41522-025-00723-9>.

Correspondence and requests for materials should be addressed to Wenfeng Li, Jun Guo, Shaokang Huang or Richou Han.

Reprints and permissions information is available at <http://www.nature.com/reprints>

Publisher's note Springer Nature remains neutral with regard to jurisdictional claims in published maps and institutional affiliations.

Open Access This article is licensed under a Creative Commons Attribution-NonCommercial-NoDerivatives 4.0 International License, which permits any non-commercial use, sharing, distribution and reproduction in any medium or format, as long as you give appropriate credit to the original author(s) and the source, provide a link to the Creative Commons licence, and indicate if you modified the licensed material. You do not have permission under this licence to share adapted material derived from this article or parts of it. The images or other third party material in this article are included in the article's Creative Commons licence, unless indicated otherwise in a credit line to the material. If material is not included in the article's Creative Commons licence and your intended use is not permitted by statutory regulation or exceeds the permitted use, you will need to obtain permission directly from the copyright holder. To view a copy of this licence, visit <http://creativecommons.org/licenses/by-nc-nd/4.0/>.

© The Author(s) 2025